Fc Optimization of Therapeutic Antibodies Enhances Their Ability to Kill Tumor Cells *In vitro* and Controls Tumor Expansion *In vivo* via Low-Affinity Activating Fcγ Receptors

Jeffrey B. Stavenhagen, Sergey Gorlatov, Nadine Tuaillon, Christopher T. Rankin, Hua Li, Stephen Burke, Ling Huang, Syd Johnson, Ezio Bonvini, and Scott Koenig

MacroGenics, Inc., Rockville, Maryland

Abstract

Monoclonal antibodies (mAb) are widely used in the treatment of non-Hodgkin's lymphoma and autoimmune diseases. Although the mechanism of action *in vivo* is not always known, the therapeutic activity of several approved mAbs depends on the binding of the Fcγ regions to low-affinity Fcγ receptors (FcγR) expressed on effector cells. We did functional genetic screens to identify IgG1 Fc domains with improved binding to the low-affinity activating Fc receptor CD16A (FcγRIIIA) and reduced binding to the low-affinity inhibitory Fc receptor, CD32B (FcγRIIB). Identification of new amino acid residues important for FcγR binding guided the construction of an Fc domain that showed a dramatically enhanced CD16A binding and greater than a 100-fold improvement in antibody-dependent cell-mediated cytotoxicity. In a xenograft murine model of B-cell malignancy, the greatest enhancement of an Fc-optimized anti-human B-cell mAb was accounted for by improved binding to FcγRIV, a unique mouse activating FcγR that is expressed by monocytes and macrophages but not natural killer (NK) cells, consistent with experimental and clinical data suggesting that mononuclear phagocytes, effector cells expressing both activating and inhibitory FcγR, are critical mediators of B-cell depletion *in vivo*. By using mice transgenic for human *CD16A*, enhanced survival was observed due to expression of *CD16A-158*^{phe} on monocytes and macrophages as well as on NK cells in these mice. The design of new generations of improved antibodies for immunotherapy should aim at Fc optimization to increase the engagement of activating FcγR present on the surface of tumor-infiltrating effector cell populations. [Cancer Res 2007;67(18):8882–90]

Introduction

Immunotherapy of cancer with monoclonal antibodies (mAb) promotes elimination of tumor cells by a variety of mechanisms. Although complement-dependent cytotoxicity, the interference with signaling pathways, or the induction of apoptosis have all been invoked, accumulated evidence suggests a major role for the engagement of Fc-γ receptors (FcγR) and the recruitment of effector cells in Fc-dependent cellular cytotoxicity events. Experimental evidence includes a study in a reconstituted nonobese diabetic/severe combined immunodeficient tumor model of human adult T-cell leukemia, which showed that improved survival after anti-CD25 immunotherapy was associated with non–natural killer cell-mediated Fcγ-dependent tumor cell killing (1). More significantly, the therapeutic outcome in patients treated with rituximab (Rituxan, a Food and Drug Administration–approved chimeric mouse/human IgG1 mAb against CD20) for non-Hodgkin's lymphoma (NHL; refs. 2, 3) or Waldenstrom's macroglobulinemia (4) correlated with the individual's expression of allelic variants of FcγRs with distinct intrinsic affinities for the Fc domain of human IgG1. In these studies, patients homozygous for the high-binding *CD16A-158*^{val} allele showed higher response rates and, in the cases of NHL, improved progression-free survival. The study by Weng and Levy (3) additionally showed a positive and independent association of response rates in rituximab-treated NHL patients with the high-binding allele of a second FcγR, CD32A (FcγRIIA). This study implicates the response to rituximab in NHL patients to cells that express CD32A, a subgroup of leukocytes that includes neutrophils and mononuclear phagocytes, but not NK cells. Consistent with this clinical observation, B-cell depletion in mice treated with an anti-CD20 mAb was independent of NK cells, but proceeded via an FcγR-dependent mechanism that required mononuclear phagocytes (5). Both human and murine mononuclear phagocytes express two low-affinity activating FcγR. Human mononuclear phagocytes, however, express CD16A and CD32A, whereas mice express FcγRIV, which shares the highest homology to human CD16A, together with a more distantly related receptor, FcγRIII (6).

Mononuclear phagocytes, but not NK cells, in both humans and mice also express CD32B (FcγRIIB), an inhibitory Fcγ receptor that functions as a threshold and negative regulator of cell activation (7). In agreement with its inhibitory role, the therapeutic activities of both an anti-Her2/neu mAb and an anti–E-cadherin mAb were amplified in mice deficient for the inhibitory receptor compared with the effect observed in wild-type (WT) mice (8, 9). These results further underscore the importance of the mononuclear phagocyte compartment and the relative balance between activating and inhibitory FcγR in antibody-mediated tumor cell depletion *in vivo*.

The optimization of the interaction between antibodies and FcγR has emerged as a promising technology to enhance the activity of therapeutic antibodies for cancer treatment. Improved binding to human low-affinity activating FcγR has been achieved through glycoengineering and mutagenesis (10–13). The latter approach has been limited to alanine scanning of surface-exposed residues (12) or mutagenesis guided by a protein structure design algorithm (13) targeting residues important for FcγR contact (14, 15). Here, we report the results of performing functional genetic screens using yeast surface display to identify novel human IgG1 Fc regions with increased binding to the low-affinity activating FcγR, CD16A, and reduced binding to CD32B, the low-affinity inhibitory

Note: Supplementary data for this article are available at Cancer Research Online (http://cancerres.aacrjournals.org/).

Requests for reprints: Jeffrey B. Stavenhagen, MacroGenics, Inc., 1500 East Gude Drive, Rockville, MD 20850. Phone: 301-354-2604; Fax: 301-251-5321; E-mail: stavenhagenj@macrogenics.com.

doi:10.1158/0008-5472.CAN-07-0696

FcγR. This approach yielded the identification of novel Fc variants greatly expanding the range of Fc residues that play specific roles in FcγR interactions. We further show that Fc domains, optimized for improved binding to human and mouse activating FcγR expressed on murine monocytes and macrophages, markedly increased the activity of a prototype therapeutic mAb in xenograft mouse models of B-cell lymphoma and in tumor models in FcγRIII-knockout mice that express the low-binding allele of human CD16A.

Materials and Methods

Cell Lines and Culture Conditions

The human tumor cell lines, HT29 (colon), SKOV3 (ovarian), and SKBR3 (breast); Daudi (Burkitt's lymphoma), Raji (Burkitt's lymphoma), and the murine tumor cell line EL4 (thymoma) were obtained from American Type Culture Collection. Daudi and Raji cells were maintained in RPMI 1640 with 10% fetal bovine serum (FBS), 4 mmol/L glutamine, 10 mmol/L HEPES, 1 mmol/L sodium pyruvate, 0.1 mmol/L nonessential amino acids, 50 μg/mL penicillin, and 100 μg/mL streptomycin. SKBR3, SKOV3, and HT29 cells were maintained in McCoy's 5A medium supplemented with 10% FBS, 4 mmol/L glutamine, 10 mmol/L HEPES, 50 μg/mL penicillin, and 100 μg/mL streptomycin. All cell lines were grown at 37°C, 5% CO_2. EL4 cells were maintained in DMEM with 10% horse serum. The EL4-CD32B cell line was generated by transfection via electroporation of CD32B cDNA cloned in the pCIneo (Promega). Cells were selected with 100 μg/mL of G418 (Life Technologies) followed by subcloning and screening of CD32B-positive cells by fluorescence-activated cell sorting analysis.

Yeast Surface Display

Yeast surface display was done as previously described (16, 17). Details of the library construction and screening criteria are included in the Supplementary Methods.

Antibody Cloning and Mammalian Expression

The murine antibody, 4D5 (18, 19), was chimerized to human IgG1. Ch4D5 heavy chain (HC) and light chain (LC) genes were cloned into pcDNA3.1 (Invitrogen), pcDNA-4D5HC, and pcDNA-4D5LC. Heavy-chain constant regions harboring Fc mutants were cloned as *Age*I/*Nhe*I fragments into linearized pcDNA-4D5HC. Additional amino acid changes were added to Fc mutants or WT IgG1 by site-directed mutagenesis (Quick Change, Stratagene). The rituximab HC and LC genes were cloned into pCIneo and pcDNA3.1, respectively. The ch4D5 HC Fc mutants were converted to rituximab by swapping the HC variable domains. Fc mutants were analyzed in the humanized anti-CD32B antibody, hu2B6 (20). Fc mutant 18 (F243L/R292P/Y300L/V305I/P396L) was cloned into hu2B6 by replacing the WT Fc region with the variant Fc domains. An Fc-null version of ch4D5 was constructed as an aglycosylated molecule by introducing a single N297Q mutation in the Fc region (20).

For transient transfections, HC and LC vectors were cotransfected into HEK 293 cells using OPTI-PRO SFM (Invitrogen) as per manufacturer's instructions. Supernatants were collected on days 3, 6, and 9. For stable transfections, CHO-S cells were seeded at 0.75×10^6 per well in 2 mL of DMEM nonselection medium with glutamine, 10% FBS/0.5× Pen-Strep overnight. After 48 h at 37°C under 5% CO_2, cells were plated for selection in 96-well plates at densities of 500, 1,000, 2,000, and 4,000 per well in 200 μL of selection medium (DMEM without glutamine, 10% dialyzed/heat inactivated FBS, 25 μmol/L MSX, 1× GSEM, and 0.5× Pen-Strep). Supernatants from both transient and stable transfections were subjected to protein A chromatography for IgG1 purification. All antibodies were concentrated and analyzed by SDS-PAGE, and protein concentrations were determined by absorbance at A_{280}. Soluble recombinant receptors secreted in the conditioned medium were captured over an IgG column and the affinity-purified receptors were analyzed by SDS-PAGE.

FcγR Cloning and Expression

Vectors for expression of human Fc receptors, expression and purification of human FcγRs have been previously described (21). For the cloning of the mouse soluble FcγR, RNA from C57BL mouse spleen was isolated and used as template for cDNA synthesis (SuperScript First-Strand cDNA Synthesis System kit, Invitrogen). Reverse transcription-PCR was done using gene-specific primers for the corresponding mouse FcγR. The extracellular domains for the receptors were fused to the mouse IgG1 Fc region containing a N297Q mutation by overlapping PCR. A signal sequence was added at the NH_2 terminal to improve secretion during protein expression in 293H cells. The FcγR-Fc fusions were cloned into pCIneo (Promega) vector at *Nhe*I-*Eco*RI sites. Expression and purification was similar to that of the human FcγR-Fc fusions (21).

BIAcore Analysis of FcγR Binding

Binding of human and mouse FcγR to the IgG1 Fc was analyzed by surface plasmon resonance using a BIAcore 3000 biosensor (BIAcore). The antigen for 4D5 (R&D Systems) was immobilized on the CM-5 sensor chip by amine coupling kit as recommended by the manufacturer. Binding experiments were done in HBS-P buffer [10 mmol/L HEPES (pH 7.4), 150 mmol/L NaCl, and 0.005% P20 surfactant]. WT or mutant antibody was captured, followed by injection of the soluble monomeric receptors CD16A-158^{val} and CD16A-158^{phe} at concentrations of 400 and 800 nmol/L, respectively, and flow rate of 50 μL/min for 30 s with dissociation time 60 s. Dimeric Fc-G2 (N297Q) fusions of human CD32B and CD32A-131^{his} were injected at 100 nmol/L. Each receptor was injected in duplicate. Regeneration of the captured antibody was done by pulse injection of 50 mmol/L glycine (pH 4) and 50 mmol/L glycine (pH 9.5) and 3 mol/L NaCl. Regeneration of antigen surface was done by pulse injection of 50 mmol/L glycine (pH 1.5). Binding responses for each soluble receptor were normalized to the level of captured WT Ch4D5 antibody. The change in stability of receptor-mutant Fc complex relatively to WT Fc was evaluated by calculation of dissociation rate constants (k_{off}) from binding curves using separate k_{off}/k_{on} fit of BIAevaluation 3.0 software. Fit was applied to 31 to 33 s segment of each binding curve and average k_{off} (s^{-1}) value was calculated for each receptor-Fc interaction.

Affinities of the soluble monomeric CD16A-158^{val} and CD16A-158^{phe} with selected mutants were obtained by injection of soluble CD16A receptor alleles in duplicate at concentrations of 0, 62.5, 125, 250, 500, 1,000, and 2,000 nmol/L for 120 s at a flow rate of 30 μL/min over immobilized ch4D5-ErbB2/Fc. Avidities of mouse FcγRII, FcγRIII, FcγRIV, and human CD32B in their dimeric forms toward selected ch4D5 mutants were obtained by receptor injections in duplicates at concentrations 0, 12.5, 25, 50, 100, and 200 nmol/L for 120 to 180 s at flow rate 30 μL/min over immobilized ch4D5-ErbB2/Fc. Binding curve at zero concentration was subtracted as a blank. Equilibrium dissociation constants (K_D) were determined by fitting of equilibrium responses to steady-state affinity model provided by BIAevaluation 3.0 software.

Antibody-Dependent Cell-Mediated Cytotoxicity

Peripheral blood mononuclear cells (PBMC) were purified from whole human blood of healthy donors and used as effector cells. The genotype of each donor was determined by DNA sequence analysis. Target cells (5×10^6 in 0.5 mL) were labeled with 100 μCi of indium (In-111; GE-Amersham) at room temperature for 30 min. Unincorporated In-111 was removed through four sequential washes with cell culture medium. Target cells were opsonized with antibody at various concentrations for 30 min at 37°C. Subsequently, cells were combined with PBMC and incubated for 18 h at 37°C, 5% CO_2. For mouse NK-enriched splenocytes, the antibody-dependent ^{111}In-release assay was done by mixing 2,500 opsonized ^{111}In-labeled target cells per well with a graded number of effector cells (100:1, 50:1, 25:1, 12:1, 6:1, 3:1, 1:1) in a U-bottomed 96-well plate for 24 h at 37°C, 5% CO_2. Supernatants were harvested and released radioactivity was quantified. Maximal release (MR) and spontaneous release (SR) were determined by incubation of target cells with 2% Triton X-100 and medium alone, respectively. Antibody-independent cellular cytotoxicity (AICC) was measured by incubation of target and effector cells in the absence of antibody. Total cytolysis was calculated as follows: (release by effector cells plus target cells − SR) / (MR − SR) × 100. The specific cytolysis is calculated as total cytolysis − AICC.

Enrichment of NK Cells from Mouse Splenocytes

Mouse spleens were crushed between glass slides in RPMI 1640. The homogenized spleen was placed on ice for 5 min. Splenocytes were spun at 1,000 rpm for 10 min. Splenocytes were resuspended in RPMI 1640 containing 10% FBS, 2 mmol/L glutamine, kanamycin (100 μg/mL), incubated with Dynabeads Mouse pan T and pan B for 30 min at 4°C and the beads together with T cells and B cells were removed. The resulting supernatant was enriched further by mixing with Dynabeads Sheep anti-rat IgG and rat anti-mouse CD24. The remaining cells (NK-enriched splenocytes) were washed and cultured in RPMI 1640 containing 10% FBS, 2 mmol/L glutamine, kanamycin (100 μg/mL), 5×10^{-5} mol/L β_2-mercaptoethanol, and 10 ng/mL human interleukin 2.

Mouse Tumor Models

Xenograft models. Female athymic BALB/c nude (nu/nu) mice, 8 to 10 weeks old, were purchased from Taconic. Daudi cells (5×10^6 per mouse) were suspended in PBS + Matrigel and injected s.c. into the right flank of BALB/c nude mice. Tumor development was monitored twice per week, using calipers, and tumor weight was estimated by the following formula: tumor weight = (length × width^2)/2. I.p. injections of antibodies at various concentrations (1 μg/g, or 0.1 μg/g) were done weekly for 7 weeks, starting at day 0.

Transgenic tumor models. Male and female athymic *mFcγRIII*$^{-/-}$, *hCD16A*$^{+}$ nude mice, were bred in MacroGenics animal facility. EL4/CD32B cells (1×10^4 per mouse) or SKOV3 (2×10^6 per mouse) were suspended in PBS and injected i.p. at day 0. I.p. injections of anti-CD32B (hu2B6) antibodies (4 μg/g) were done on days 0, 1, 2, and 3. I.p. injections of anti-HER2 (ch4D5) antibodies (4 μg/g) were done on day 0 and continued weekly for 7 weeks. Mouse body weight was measured twice a week. Mice showing excessive body weight gain as well as signs of ascites were sacrificed by CO_2 asphyxiation. Survival was recorded accordingly. Animal studies were conducted in accordance with the Public Health Service Policy on the Humane Care and Use of Laboratory Animals. Data was analyzed using PRISM (Graphpad Software) for calculation of SD [antibody-dependent cell-mediated cytotoxicity (ADCC), tumor model] and statistical significance using *t* tests and log-rank analysis (tumor models).

Results

Selection and binding analysis of IgG1 Fc variants. We undertook a comprehensive functional genetic screen of the IgG1 Fcγ region to elucidate the contribution of different amino acid residues to the binding to low-affinity FcγR. Yeast surface display (16, 22) was done on a random library of $\sim 1 \times 10^7$ Fc mutants by using both equilibrium and kinetic screening strategies for binding to a phycoerythrin-conjugated soluble CD16A, CD32A, and/or CD32B as ligands (Supplementary Methods). The "single round" approach yielded Fc domains with enhanced avidity for the low-affinity activating FcγR, CD16A. To enrich the IgG1 Fc library for Fc variants with limited or no binding potential to the inhibitory receptor, CD32B, the library was first absorbed to beads coated with recombinant CD32B, followed by amplification of the remaining yeast cells and positive selection for binding to either activating receptor, CD16A or CD32A. The "dual round" strategy was highly reiterative, resulting in an enriched population of yeast cells harboring a limited number of Fc mutants, with reduced binding to the inhibitory receptor, CD32B, and at least WT binding to CD16A.

In total, over 400 amino acid changes were identified from Fcγ mutant libraries spanning both the CH2 and CH3 domains (Fig. 1*A* and *B*; Supplementary Data). The nonrestrictive nature of our strategy enabled the identification of residues previously unknown to mediate molecular interactions within the Fcγ domain or effect on the kinetics of Fcγ/FcγR interactions. Novel Fc variants were selected containing multiple mutations that had significant effects on FcγR binding. Analysis of the collection of single- and multiple-site mutants selected by yeast display revealed that specific mutations recurred frequently, a potential indication of the importance of an individual residue for FcγR binding (Fig. 1*A* and *B*; Supplementary Data). The most frequently identified sites in the single round (326, 334, 396) and dual round screening (270, 292, 298, 330, 396) included sites that had also been identified by alanine-scanning mutagenesis as important for FcγR binding (326, 334, 270, 292, 298, 330; ref. 12), validating the use of yeast surface display as a functional tool for selection of Fc regions with increased binding to FcγR.

Comparison of off-rates (k_{off}) for selected Fc mutants, single amino acid changes, or Fc domains containing multiple mutations was done to identify an Fc domain optimized for improved binding to the activating receptors and reduced binding to CD32B. Off-rate analysis provides the best indicator for potential improvement of *in vivo* FcγR binding activity because as a kinetic variable it directly reflects the Fc-FcγR interaction independent of antibody concentration (23). Fc-engineered versions of ch4D5, the progenitor to the anti-HER2/neu antibody, trastuzumab (Herceptin; ref. 19), were analyzed by surface plasmon resonance for k_{off} to confirm the improvement in binding of Fc variants in the context of a native antibody. Fc variant 13, selected during the dual round screen, showed a dramatic reduction in binding to CD32B. Analysis of each of the amino acid changes in mutant 13 as a single and in some cases a double mutant indicated that the reduction in binding to CD32B was due mostly to amino acid changes at positions R292P and F243L with a context-dependent contribution of V305I (Table 1). Next, we constructed novel Fc variants by grouping different amino acid substitutions identified in the functional screen to determine which combination of mutations would provide the greatest overall improvement in off-rate to CD16A (Table 1). Fc variants 16 (F243L/R292P/Y300L/P396L) and 18 (F243L/R292P/Y300L/V305I/P396L) showed the overall greatest improvement in off-rate to both the high-affinity (158^{val}) and low-affinity (158^{phe}) isoform of CD16A and CD32A-131^{His} while maintaining approximately WT binding to CD32B. In contrast, two mutants, 12 (F243L/R292P/Y300L) and 14 (F243L/R292P/P396L), showed an improvement in binding to CD16A and a reduction in binding to CD32B. Fc variant 18, with the greatest improvement in off-rate to CD16A, did not show a significant improvement in binding to the human CD64, the high-affinity activating FcγR (data not shown).

Fc variants with increased ADCC. The biological effect of enhancing FcγR binding was examined in three different antibodies. Fc-engineered versions of ch4D5 were tested against a HER2/neu^{+} colon carcinoma cell line, HT29 (Fig. 2*A*). In general, Fc mutants with slower off-rates for CD16A showed greater increases in ADCC (Table 1; Fig. 2*A*) and, within a limited set of four Fc, ADCC improvement showed a direct relationship with affinity for CD16A (Table 2; data not shown). An absolute correlation between CD16A off-rates and ADCC, however, was not observed, owing to some exceptions with slower off-rates that show no ADCC improvement. These exceptions suggest that other interactions may be important for mediating this complex function. Two mutants, 18 (F243L/R292P/Y300L/V305I/P396L) and 12 (F243L/R292P/Y300L), mediated the highest levels of ADCC, showing an ~100-fold increased rate of lysis, as noted by a leftward shift in the curve and an increase in maximal lysis. Of these two Fc variants, variant 18 showed a greater effect on specific lysis at lower antibody concentrations (Fig. 2*B*). Genotyping for the *CD16A-158* polymorphism further showed that variant 18 was also remarkably effective in improving ADCC from the low binding *CD16A-158*^{phe}

allele carriers (Fig. 2*C*). In addition to HT29 (colon; $\sim 10^4$ copies per cell), Ch4D5-18 also enhanced ADCC against SKOV3 (ovarian; $\sim 10^6$ copies per cell) and SKBR3 (breast; $\sim 5 \times 10^6$ copies per cell) tumor cell lines (Fig. 2*A* and *D*; refs. 18, 24), indicating that variant 18 improves ch4D5-mediated ADCC irrespective of the level of HER2/neu expression or tissue origin of the target cells. We analyzed Fc variants 18 and 12 in the anti-CD20 mAb, rituximab (25), to determine if the Fc optimization enhanced the activity of different antibodies. Both variants exhibited enhanced ADCC against the human Burkitt's lymphoma line, Daudi, at multiple antibody concentrations (Fig. 3*A*). Variant 18 was also used to increase effector function in a third antibody, a humanized version of a novel anti-CD32B mAb (20), that has been shown to be effective in treatment of xenograft models for B-cell malignancies. Hu2B6-18 increased ADCC in an antibody concentration–dependent fashion against two different human Burkitt's lymphoma lines, Daudi and Raji, using PBMC from multiple donors (Fig. 3*B*).

The availability of transgenic murine models expressing human FcγR provides a unique opportunity to evaluate the ability of Fc engineering to enhance the potency of therapeutic antibodies *in vivo*. The activity of Fc-engineered mAbs was analyzed using effector cells from mFcγRIII-knockout mice expressing the transgene for the low-affinity allele of human CD16A (26). In these mice, human *CD16A-158*^{phe} is expressed by NK cells and mononuclear phagocytes, similarly to its cell type–specific expression in humans (27). *In vitro* ADCC using harvested splenocytes from WT BALB/c, BALB/c *FcγRIIIA*$^{-}$, and BALB/c *mFcγRIIIA*$^{-}$ *hCD16A-158*^{phe} mice strains was used to characterize the potential of these mice to mediate Fc-dependent lysis of Daudi cells via a human IgG antibody. Only splenocytes harvested from the *hCD16A-158*^{phe} transgenic mice were able to mediate ADCC (Fig. 3*C*). As predicted from studies with human PBMC, hu2B6-18 showed a significantly greater level of lysis compared with hu2B6-WT.

Fc optimization improves survival in a xenograft tumor model for ovarian cancer. Fc optimization of ch4D5, an antibody that is capable of mediating tumor depletion by multiple mechanisms, including ADCC and tumor cell growth inhibition (8, 28), was evaluated in an ovarian tumor model expressing high levels of HER2/neu antigen. We assayed Fc-optimized ch4D5 antibodies in the *hCD16A-158*^{phe} transgenic mice injected with SKOV3, an ovarian carcinoma cell line. Mice treated with variant ch4D5-18 showed significant enhancement in protection over the

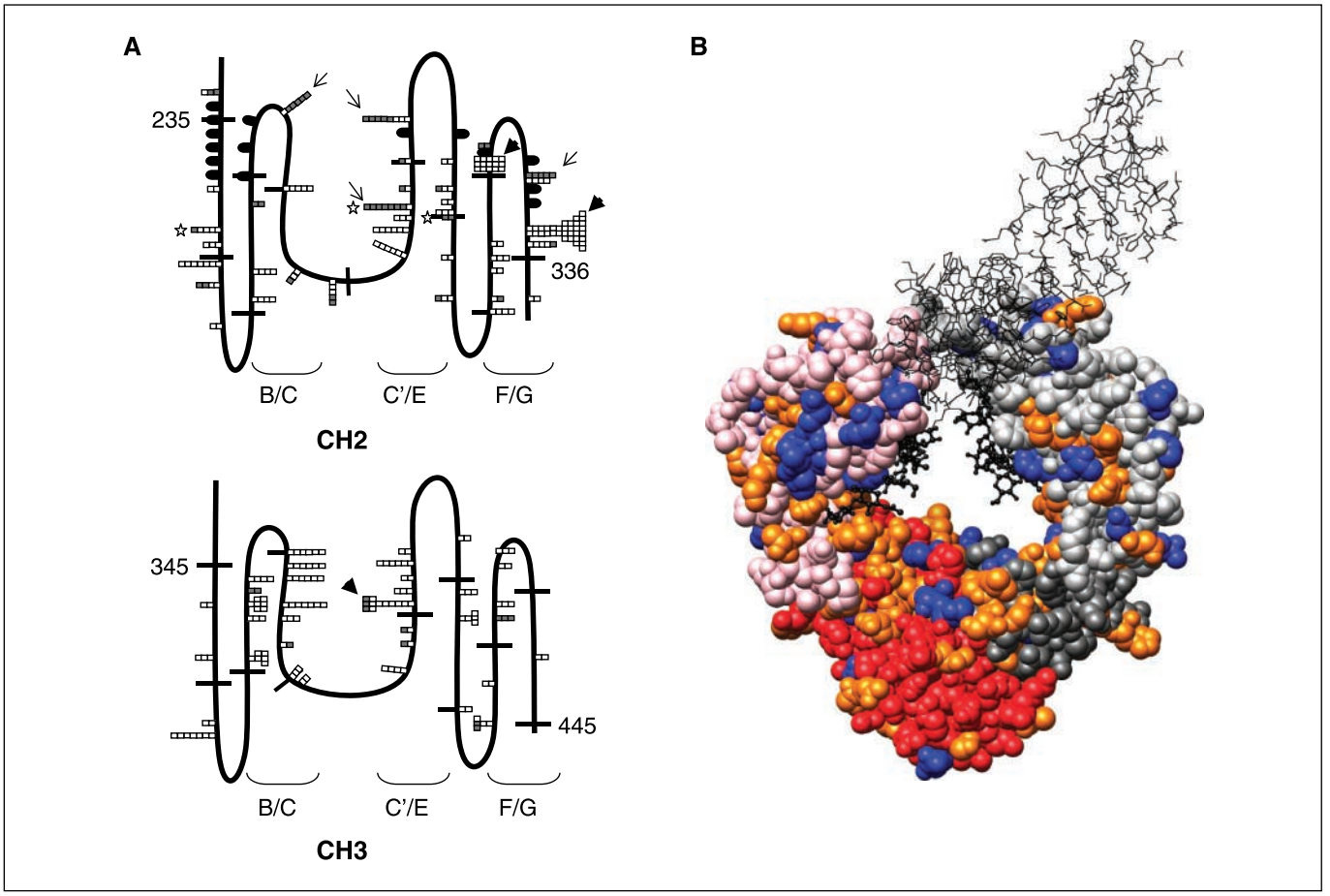

Figure 1. Locations of Fc mutations identified by yeast surface display. *A,* two-dimensional Collier de Perles representations of the IgG1 CH2 and CH3 domains (39). *Black semiovals,* FcγRIIIB (CD16B)-IgG Fc contact residues (15). *Open boxes,* amino acid changes identified in single round screens; *shaded boxes,* residues identified in dual round screens. Specific frequently identified residues are marked from the single round screen: 326, 334, and 396 (*large arrowheads*); the dual round screen: 270, 292, 298, 330 (*arrows*); and amino acids 243, 292, and 305 (*stars*) mutated in variant 13. Perpendicular lines are placed at 10 amino acid intervals. *B,* space-filling diagram of the IgG1 Fc-FcγRIIIB cocrystal structure (15). The positions of the amino acid changes in the single round and dual round screens are indicated in orange and blue, respectively. In cases where the amino acid variant was identified in both screens, the residue is marked as blue. The α-chain (*gray*) and β-chain (*red*) are color coded, and the CH2 (*lighter shade*) and CH3 (*darker shade*) are identified. The ball-and-stick structures represent the N-linked carbohydrate moiety and the wireframe structure represents FcγRIIIB.

Table 1. Comparison of k_{off} of Fc mutants to WT Fc (WT/mutant)

Fc mutant (MG no.)	Amino acid changes							CD16A^{V}	CD16A^{F}	CD32A^{H}	CD32B
Single amino acid											
1	F243L							**4.8**	**3.4**	**0.6**	0.8
2		D270E						1.3	1.5	**2.2**	**0.4**
3			R292P					**2.4**	1.6	0.7	**0.3**
4				S298N				nd	nd	nt	**0.2**
5					Y300L			1.0	1.2	**2.9**	1.2
6						V305I		0.9	0.6	1.3	1.2
7							A330V	0.6	1.2	**0.4**	**0.3**
8							P396L	1.3	1.7	1.6	**2.6**
Two amino acids											
9	F243L						P396L	**2.2**	**2.0**	1.5	1.6
10	F243L		R292P					**4.0**	1.7	**0.5**	**0.2**
11			R292P			V305I		1.3	1.3	0.8	**0.4**
Three amino acids											
12	F243L		R292P		Y300L			**7.4**	**4.6**	1.0	0.6
13	F243L		R292P			V305I		**2.6**	1.4	**0.2**	**0.1**
14	F243L		R292P				P396L	**6.3**	**3.4**	1.4	**0.4**
15			R292P			V305I	P396L	**1.9**	**1.9**	1.5	0.9
Four amino acids											
16	F243L		R292P		Y300L		P396L	**10.1**	**5.6**	1.7	1.1
17	F243L		R292P			V305I	P396L	**4.0**	**2.3**	0.8	**0.4**
Five amino acids											
18	F243L		R292P		Y300L	V305I	P396L	**10.1**	**8.3**	**3.2**	1.4

NOTE: Human CD16A has intermediate affinity to human IgG1 because it shows measurable binding to monomeric IgG1 Fc. In contrast, the low-affinity receptors hCD32A and hCD32B do not show measurable binding to monomeric human IgG1. These FcγR were expressed in their dimeric forms because, due to avidity effect, they show measurable binding to captured hIgG1. Dissociation rate constants for binding to the different FcγR were determined by BIAcore analysis and directly compared with WT Fc (x = WT k_{off}/mutant k_{off}). Values with ≥80% difference (≥0.8-fold) from WT in either direction are in bold. Shading denotes Fc mutants identified directly by yeast display; all other mutants were constructed by site-directed mutagenesis.

Abbreviations: nd, no detectable binding; nt, not tested.

same dosing regimen of ch4D5-WT antibody (Fig. 4*A*). Ch4D5-WT showed significant improvement compared with either PBS or an Fc null version of ch4D5 (aglycosylated) controls, with 15% of mice surviving until the end of the experiment compared with 100% mortality by day 100. However, animals treated with ch4D5-18 showed the greatest rate of survival, 40% survival through the duration of the experiment. These data indicate that the greatly enhanced tumor cell killing observed *in vitro* translates to dramatic improvement in tumor clearance *in vivo* and the Fc dependency of the anti-HER2 mAb therapeutic response in this model system.

Enhanced tumor clearance in B-cell tumor models with Fc-optimized mAbs. The effect of Fc engineering on tumor clearance was investigated by using WT or human FcγR-transgenic mice. Hu2B6 was used because this antibody does not induce complement lysis or apoptosis, but inhibits tumor growth in mice by mechanisms that are exquisitely FcγR dependent (20). Because hu2B6 does not cross-react with murine FcγRII or other endogenous murine proteins, there is no antibody target other than the implanted CD32B-positive tumor cells in this model. Furthermore, hu2B6 completely blocks human CD32B (20, 21), thus eliminating binding of the hu2B6 Fc region to the target cells as a confounding factor.

To evaluate the functional consequences of our Fc mutations in an *in vivo* murine model, the binding profiles of the engineered Fcγ to the mouse FcγR were fully characterized. Of the mFcγR, mFcγRII is structurally and functionally homologous to human CD32B, whereas mFcγRIII and mFcγRIV are receptors functionally related to human activating FcγR expressed on NK cells and monocyte/macrophages, respectively (29, 30). Mutant 18 showed increased binding primarily to mFcγRIV, with no increase in binding to the inhibitory receptor (Table 2).

S.c. inoculation of Daudi cells in nude mice produced localized, progressively expanding tumors whose growth was significantly reduced by weekly i.p. injections of 1 μg/g hu2B6-WT. A 10-fold reduction in dose of hu2B6-WT, however, was completely ineffective (Fig. 4*B*). Treatment with hu2B6-18 resulted in a significant reduction in tumor growth at all doses tested, consistent with its enhanced mFcγRIV binding.

For the *in vivo* study in the *mFcγRIIIA*$^{-}$ *hCD16A-158*^{phe} mice, the murine cell line EL4 (31) was transduced with human CD32B and used in place of Daudi cells, whose tumor growth was poor in these transgenic mice (data not shown). Knockout transgenic mice, *mFcγRIII*$^{-/-}$*/CD16A-158*$^{phe+}$, injected i.p. with CD32B-EL4 cells, died 8 weeks after inoculation. A regimen of hu2B6-WT did not prevent tumor growth. In contrast, treatment with hu2B6-18 resulted in 100% survival for the duration of the experiment (Fig. 4*C*). Therefore, the potency of hu2B6-18 *in vivo* is consistent with the relative improvement in binding to FcγR expressed in the mice (Table 2). Furthermore, variant 18 is able to improve survival in both the EL4 and ovarian cancer models.

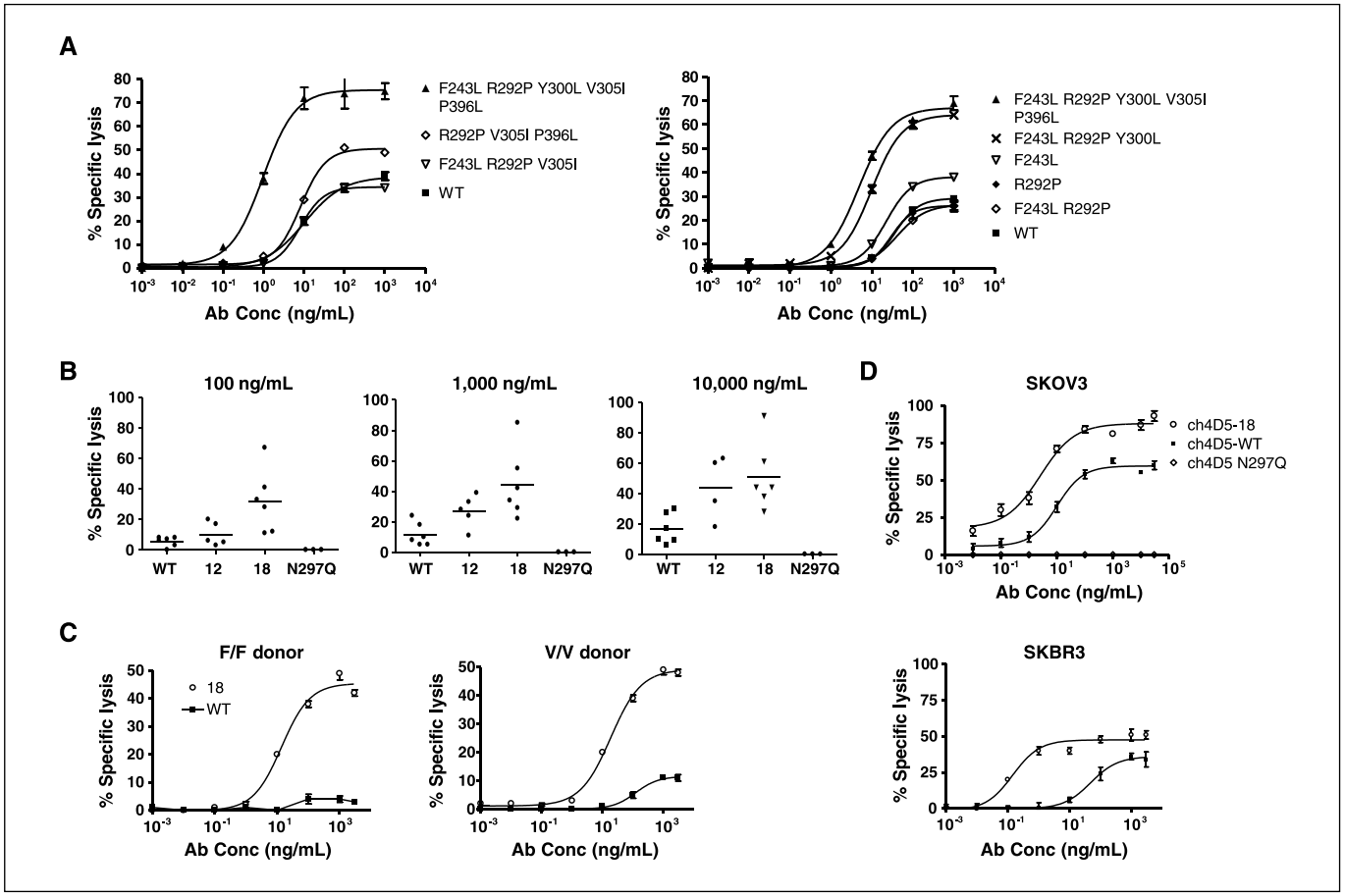

Figure 2. Fc optimization of ch4D5 enhances ADCC activity. *A,* ADCC assays were done using HT29 target cells incubated with PBMC from CD16A 158^{phe} carrier donors in the presence of ch4D5 WT or ch4D5 containing Fc variants. Individual assays were done in triplicate at an effector-to-target ratio of 50:1. Data are plotted using nonlinear regression analysis. *B,* compilation of ADCC data for ch4D5 comparing WT to variants 12, 18, and N297Q at three different concentrations. Assays were done as described above. For each variant, three or more independent assays are plotted. *Black line,* mean percentage specific lysis. *C,* comparison of ADCC data using HT29 target cells incubated with PBMC from either *CD16A-158*$^{val/val}$ or *CD16A-158*$^{phe/phe}$ homozygous donors. *D,* analysis of ch4D5-WT and ch4D5-18–mediated ADCC against target cells. *A, C*, and *D,* representative plots of at least three independent assays.

Discussion

We have identified several key positions in the human IgG1 Fc region whose permutations generate Fc domains customized to a predefined FcγR-binding profile, including conferring the ability to engage the low-binding CD16A-158^{phe} allele with enhanced ADCC *in vitro* and increased tumor elimination *in vivo*. Together with data that show the portability of the Fc-optimized mutant portfolio to mAbs of different specificities, this evidence contributes to

Table 2. Binding of Fc variants to murine and human FcγRs

	Affinity measurements (K_D, nmol/L)					
	Human Fc receptors			Murine Fc receptors		
	CD16A-158^{val}	CD16A-158^{phe}	CD32B	mFcRII	mFcRIII	mFcRIV
WT	411 (403–419)	1,066 (981–1150)	33 (25–41)	84 (80–87)	157 (144–169)	79 (67–90)
18	40 (32–48)	99 (77–121)	17 (16–17)	106 (91–121)	113 (106–120)	19 (18–19)

NOTE: The low-affinity receptor hCD32B and the mouse FcγRs do not show measurable binding to monomeric human IgG1. These FcγRs were expressed in their dimeric forms because, due to avidity effect, they show measurable binding to captured hIgG1. In the case of dimeric forms of the receptors, equilibrium dissociation constant (K_D) represents a relative avidity value that was used for assessment of the relative effect of mutations on the receptor binding to Fc. The average K_D was based on at least two independent measurements; ranges are shown in parenthesis.

establishing Fc engineering as a robust means of optimizing mAbs for therapeutic enhancement.

A functional genetic screen of a random mutant library covering both CH2 and CH3 domains allowed us to identify several amino acid substitutions that had not been predicted to affect FcγR binding from crystallographic analyses or in previous mutagenesis studies. Previously, Fc variants with increased binding to CD16A were identified by alanine scanning mutagenesis or a protein structure design algorithm (S298A, E333A, K334A and S239D, I332E, A330L), respectively (12, 13). These approaches limited the search to soluble residues or amino acid positions that were direct Fc-FcγR contact sites or residues in its immediate proximity (15). Interestingly, alanine scanning identified a number of soluble residues within both the CH2 and CH3 domain that were not predicted to affect Fc-FcγR binding (12). The Fc mutations selected by yeast surface display contain several amino acid substitutions that could only be ascertained to alter FcγR binding through a functional genetic screen (Fig. 1*B*). In particular, P396 in the CH3 domain is not a soluble residue nor does it directly interact with the FcγR, suggesting that these residues affected ligand binding via distant conformational changes. Position F243 directly contacts the carbohydrate moiety and affects sialylation of the oligosaccharide chains potentially affecting the Fc domain quaternary structure (32, 33). Two soluble residues were previously analyzed by alanine substitutions: V305 showed no change in binding to any of the low-affinity receptors and R292 only partially reduced binding to CD32A (12). Variant 18, containing substitutions at all four of these residues plus Y300L, has a dramatic increase in binding to both alleles of CD16A. The individual mutations found in variant 18, however, have different effects on FcγR binding, ranging from an increase in CD16A interaction with no change in CD32B binding to modest change in CD16A binding with a decrease in CD32B binding (Table 1). The potential to screen large Fc mutant libraries by yeast surface display allows for the identification of a suite of Fc domains with desired aggregate FcγR binding specificities.

The ability of a mutant to bind CD16A correlated in general with its capacity to mediate *in vitro* cytotoxic activity. Single amino acid Fc variants showed limited improvement in CD16A off-rates, but resulted in no improved ADCC, consistent with previously published data (12). Fc variant 18 showed the greatest increase in binding to CD16A and mediated a ~100-fold improvement in ADCC in the context of three different mAb backbones. Furthermore, the ability of variant 18 to enhance ADCC in a *CD16A* allele-independent fashion suggests potential applications of this optimized Fc domain in patients who carry the low-binding allele of this receptor. The correlation between *in vitro* ADCC and tumor depletion *in vivo*, however, can only be partial, because the primary mediators of cytotoxicity in PBMC-based ADCC are NK cells, leukocytes that express CD16A as their sole FcγR, whereas mononuclear phagocytes expressing the whole array of activating

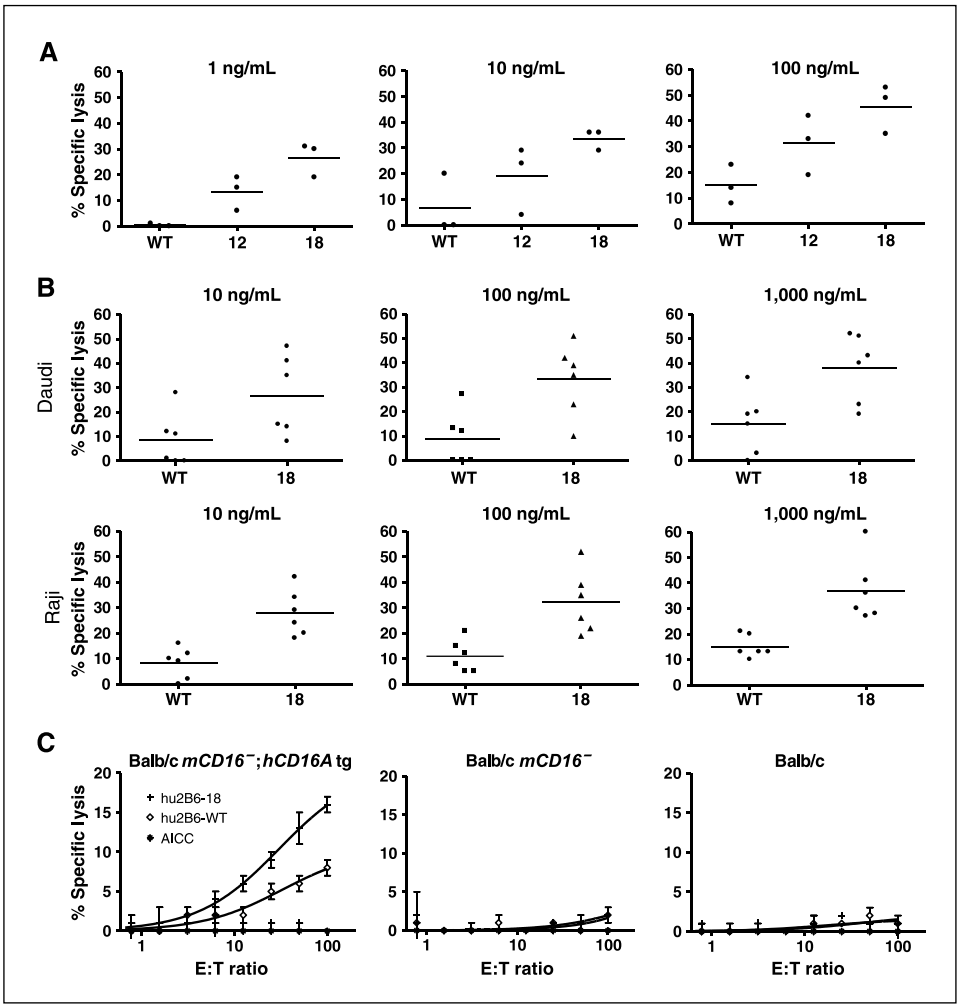

Figure 3. Fc-optimized anti-CD20 and anti-CD32B antibodies have improved ADCC against B-cell targets. *A,* compilation of ADCC data for Fc-engineered versions of rituximab comparing WT to variants 12 and 18 at different antibody concentrations. Three independent assays were done using Daudi cells as targets and PBMC from *CD16A-158*^{phe} carriers as donors at an effector-to-target ratio of 75:1. *B,* compilation of ADCC data comparing hu2B6-WT to hu2B6-18. Target cells, Daudi and Raji, were opsonized with a range of antibody concentrations and incubated with PBMC from healthy donors carrying the *CD16A-158*^{phe} allele at an effector-to-target ratio of 75:1. Six independent assays are plotted. *Black line,* mean percentage specific lysis. *C, in vitro* ADCC using splenocytes harvested from *mFcγRIII*$^{-/-}$ human *CD16A*$^{+}$ BALB/c, *mFcγRIII*$^{-/-}$ BALB/c, and BALB/c mice strains. *E:T ratio,* effector-to-target ratio.

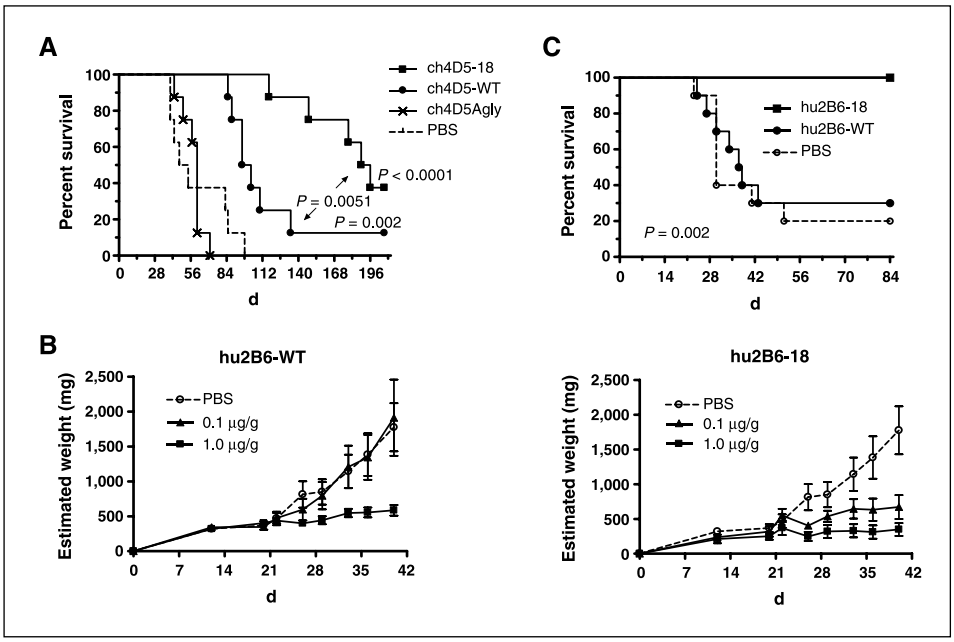

Figure 4. Fc optimization improves survival and enhances tumor-cell depletion in mouse xenograft tumor models for ovarian cancer and B-cell malignancy. *A,* ovarian cancer model: *mFcγRIII*$^{-/-}$ human *CD16A*$^{+}$ FoxN1 mice injected i.p. with SKOV3 cells (20 mice per group) and treated with ch4D5-WT, ch4D5-18, ch4D5-agly, or PBS. For all antibodies, treatment (4 μg/g) was weekly for 7 wks starting on day 0. Data were analyzed for significance using log-rank analysis. *B,* BALB/c FoxN1 (nu/nu) mice (six to eight mice per group) were injected s.c. with Daudi cells. Starting on day 0, mice were treated weekly for 7 wks with either hu2B6-WT or hu2B6-18 at two different concentrations of antibody (0.1 or 1 μg/g). Tumor growth was monitored over time (*X axis*) and the calculated tumor size was recorded (*Y axis*). *C,* Kaplan-Meier survival plots of *mFcγRIII*$^{-/-}$ human *CD16A*$^{+}$ FoxN1 mice injected i.p. with CD32B-EL4 cells (10 mice per group) and treated with either hu2B6-WT or Fc-engineered hu2B6-MG18 (4 μg/g) on days 0, 1, 2, and 3. Data were analyzed for significance using log-rank analysis.

and inhibitory FcγRs (34–36) have been shown to play an important role in cell depletion *in vivo* (5). Therefore, the complex balance of activating and inhibitory functions on the activity of Fc-optimized mAbs can only be appreciated in *in vivo* models.

A recent study showed increased B-cell depletion in *cynomologous* macaques treated with an anti-CD20 mAb engineered for improved human CD16A binding (13) and presumably macaque FcγR, albeit no direct measurement was provided. Because in primates both NK cells and monocytes express CD16A, the precise mechanism contributing to the enhanced depletion could not be ascertained. The presence in mice of a unique FcγR differentially expressed between NK cells and mononuclear phagocytes allows, albeit indirectly, to dissect the roles of these populations in the enhanced activity of Fc-optimized mAbs. Although mFcγRIII is expressed on mononuclear phagocytes, neutrophils, and NK cells, mFcγRIV, a receptor with no corresponding human homologue, is expressed by mononuclear phagocytes and a subset of neutrophils, but not NK cells (30). Mouse mononuclear phagocytes also express the inhibitory receptor, mFcγRII, the homologue of human CD32B. The hu2B6-18 mAb is more effective than hu2B6-WT in preventing tumor growth in WT mice (Fig. 4*B*). The properties of Fc variant 18, an Fcγ domain with increased affinity to mFcγRIV but mFcγRIII-binding properties similar to those of WT Fc, is consistent with the notion that mononuclear phagocytes are critical for improved tumor elimination *in vivo* (36). This notion is further supported by data demonstrating that NK cells enriched from mouse splenocytes show no ADCC *in vitro* with any form of hu2B6 mAb unless they express the hCD16A transgene (Fig. 3*C*), in which case the activity was enhanced by Fc optimization. In the huFcγR transgenic mouse (26), replacement of mFcγRIII with huCD16A-158^{phe} on both NK cells and monocytes resulted in mice expressing two activating receptors for which Fc variant 18 has increased affinity. The greater increase in mouse survival in both the B-cell tumor and ovarian tumor correlated with increased affinity of variant 18 for both huCD16A-158^{phe} expressed on both NK cells and monocyte/macrophages and mFcγRIV, expressed exclusively by mononuclear phagocytes (29). Furthermore, the enhanced *in vivo* antitumor activity of Fc variant 18 correlated with an increased affinity to mFcγRIV with no change in binding to mFcγRII (Table 2). Improvement in the activating-to-inhibitory binding ratio of the Fc region has been proposed as a critical variable in optimizing therapeutic antibodies that mediate tumor cell killing via monocyte/macrophage effector cells (29). These data suggest that strategies aimed at improving human tumor immunotherapy via enhanced FcγR engagement should focus on the mononuclear phagocyte compartment and its array of FcγRs.

Increasing the activity of antibodies for cell-depleting applications can potentially reduce the immunotherapeutic dose and confer activity to an antibody with limited *in vivo* effectiveness. In addition, Fc optimization can be tailored to certain FcγRs and used for immunotherapies ranging from autoimmunity to allergy or the treatment of infectious disease. For instance, selectively increasing CD32A binding may enhance phagocytosis and have broad applications in antibacterial therapeutics, given the predominant role of this receptor in infectious diseases (37, 38). Future studies will focus on exploiting the properties of antibodies with these optimized Fcγ domains. Alterations in the Fc could also affect the half-life of these molecules by altering their binding to the neonatal FcR (FcRn); however, BIAcore and pharmacokinetic analyses in rats indicated that the five mutations incorporated into Fc variant 18 did not affect binding to FcRn or half-life, respectively (data not shown). As with other means of protein modification, the potential effect of specific mutations on the immunogenicity of the resulting molecule in humans will need to be established and this risk evaluated in the context of the benefit of increasing the antibody therapeutic window and of expanding treatment opportunities to patients that would otherwise poorly respond to immunotherapy.

Acknowledgments

Received 2/22/2007; revised 5/10/2007; accepted 7/6/2007.

The costs of publication of this article were defrayed in part by the payment of page charges. This article must therefore be hereby marked *advertisement* in accordance with 18 U.S.C. Section 1734 solely to indicate this fact.

We thank Yanira Manzanarez, Shannon Thomas, Valentina Ciccarone, Weili Wang, Kalpana Shah, and Qin Zhou for expert technical assistance. We also thank Dr. Jeffrey Ravetch for his intellectual contributions. Molecular graphics images were produced using the University of California, San Francisco, Chimera package from the Resource for Biocomputing, Visualization, and Informatics at the University of California, San Francisco (supported by NIH P41 RR-01081).

Several of the authors (J.B. Stavenhagen, S. Gorlatov, N. Tuaillon, C.T. Rankin, H. Li, S. Burke, L. Huang, S. Johnson, E. Bonvini, and S. Koenig) are employed by MacroGenics, Inc., whose (potential) product was studied in the present work. Additionally, several of the authors (J.B. Stavenhagen, S. Gorlatov, C.T. Rankin, N. Tuaillon, L. Huang, S. Johnson, E. Bonvini, and S. Koenig) have filed patent applications related to the work that is described in the present study.

References

1. Zhang M, Zhang Z, Garmestani K, et al. Activating Fc receptors are required for antitumor efficacy of the antibodies directed toward CD25 in a murine model of adult T-cell leukemia. Cancer Res 2004;64:5825–9.

2. Cartron G, Dacheux L, Salles G, et al. Therapeutic activity of humanized anti-CD20 monoclonal antibody and polymorphism in IgG Fc receptor FcγRIIIa gene. Blood 2002;99:754–8.

3. Weng WK, Levy R. Two immunoglobulin G fragment C receptor polymorphisms independently predict response to rituximab in patients with follicular lymphoma. J Clin Oncol 2003;21:3940–7.

4. Treon SP, Hansen M, Branagan AR, et al. Polymorphisms in FcγRIIIA (CD16) receptor expression are associated with clinical response to rituximab in Waldenstrom's macroglobulinemia. J Clin Oncol 2005;23:474–81.

5. Uchida J, Hamaguchi Y, Oliver JA, et al. The innate mononuclear phagocyte network depletes B lymphocytes through Fc receptor-dependent mechanisms during anti-CD20 antibody immunotherapy. J Exp Med 2004;199:1659–69.

6. Nimmerjahn F, Ravetch JV. Fcγ receptors: old friends and new family members. Immunity 2006;24:19–28.

7. Ravetch JV, Bolland S. IgG Fc receptors. Annu Rev Immunol 2001;19:275–90.

8. Clynes RA, Towers TL, Presta LG, Ravetch JV. Inhibitory Fc receptors modulate *in vivo* cytotoxicity against tumor targets. Nat Med 2000;6:443–6.

9. Green SK, Karlsson MC, Ravetch JV, Kerbel RS. Disruption of cell-cell adhesion enhances antibody-dependent cellular cytotoxicity: implications for antibody-based therapeutics of cancer. Cancer Res 2002;62:6891–900.

10. Umana P, Jean-Mairet J, Moudry R, Amstutz H, Bailey JE. Engineered glycoforms of an antineuroblastoma IgG1 with optimized antibody-dependent cellular cytotoxic activity. Nat Biotechnol 1999;17:176–80.

11. Shinkawa T, Nakamura K, Yamane N, et al. The absence of fucose but not the presence of galactose or bisecting *N*-acetylglucosamine of human IgG1 complex-type oligosaccharides shows the critical role of enhancing antibody-dependent cellular cytotoxicity. J Biol Chem 2003;278:3466–73.

12. Shields RL, Namenuk AK, Hong K, et al. High resolution mapping of the binding site on human IgG1 for FcγRI, FcγRII, FcγRIII, and FcRn and design of IgG1 variants with improved binding to the FcγR. J Biol Chem 2000;276:6591–604.

13. Lazar GA, Dang W, Karki S, et al. Engineered antibody Fc variants with enhanced effector function. Proc Natl Acad Sci U S A 2006;103:4005–10.

14. Radaev S, Motyka S, Fridman WH, Sautes-Fridman C, Sun PD. The structure of a human type III Fcγ receptor in complex with Fc. J Biol Chem 2001;276:16469–77.

15. Sondermann P, Huber R, Oosthuizen V, Jacob U. The 3.2-A crystal structure of the human IgG1 Fc fragment-Fc γRIII complex. Nature 2000;406:267–73.

16. Boder ET, Wittrup KD. Yeast surface display for screening combinatorial polypeptide libraries. Nat Biotechnol 1997;15:553–7.

17. Boder ET, Wittrup KD. Yeast surface display for directed evolution of protein expression, affinity, and stability. Methods Enzymol 2000;328:430–44.

18. Hudziak RM, Lewis GD, Winget M, Fendly BM, Shepard HM, Ullrich A. p185HER2 monoclonal antibody has antiproliferative effects *in vitro* and sensitizes human breast tumor cells to tumor necrosis factor. Mol Cell Biol 1989;9:1165–72.

19. Carter P, Presta L, Gorman CM, et al. Humanization of an anti-p185HER2 antibody for human cancer therapy. Proc Natl Acad Sci U S A 1992;89:4285–9.

20. Rankin CT, Veri MC, Gorlatov S, et al. CD32B, the human inhibitory Fc-{γ} receptor IIB, as a target for monoclonal antibody therapy of B-cell lymphoma. Blood 2006;108:2384–91.

21. Veri MC, Gorlatov S, Li H, et al. Monoclonal antibodies capable of discriminating the human inhibitory Fcγ-receptor IIB (CD32B) from the activating Fcγ receptor IIA (CD32A): biochemical, biological, and functional characterization. Immunology 2007;129:392–404.

22. Wittrup KD. Protein engineering by cell-surface display. Curr Opin Biotechnol 2001;4:395–9.

23. Gurbaxani BM, Morrison SL. Development of new models for the analysis of Fc-FcRn interactions. Mol Immunol 2006;43:1379–89.

24. Shawver LK, Mann E, Elliger SS, Dugger TC, Arteaga CL. Ligand-like effects induced by anti-c-erbB-2 antibodies do not correlate with and are not required for growth inhibition of human carcinoma cells. Cancer Res 1994;54:1367–73.

25. Reff ME, Carner K, Chambers KS, et al. Depletion of B cells *in vivo* by a chimeric mouse human monoclonal antibody to CD20. Blood 1994;83:435–45.

26. Li M, Wirthmueller U, Ravetch JV. Reconstitution of human FcγRIII cell type specificity in transgenic mice. J Exp Med 1996;183:1259–63.

27. Perussia B, Ravetch JV. FcγRIII (CD16) on human macrophages is a functional product of the FcγRIII-2 gene. Eur J Immunol 1991;21:425–9.

28. Baselga J, Norton L, Albanell J, Kim YM, Mendelsohn J. Recombinant humanized anti-HER2 antibody (Herceptin) enhances the antitumor activity of paclitaxel and doxorubicin against HER2/neu overexpressing human breast cancer xenografts. Cancer Res 1998;58:2825–31.

29. Nimmerjahn F, Ravetch JV. Divergent immunoglobulin γ subclass activity through selective Fc receptor binding. Science 2005;310:1510–2.

30. Nimmerjahn F, Bruhns P, Horiuchi K, Ravetch JV. FcγRIV: a novel FcR with distinct IgG subclass specificity. Immunity 2005;23:41–51.

31. Gorer PA. Studies in antibody response of mice to tumor inoculation. Br J Cancer 1950;4:372–9.

32. Deisenhofer J. Crystallographic refinement and atomic models of a human Fc fragment and its complex with fragment B of protein A from *Staphylococcus aureus* at 2.9- and 2.8-A resolution. Biochemistry 1981;20:2361–70.

33. Lund J, Takahashi N, Pound JD, Goodall M, Jefferis R. Multiple interactions of IgG with its core oligosaccharide can modulate recognition by complement and human Fcγ receptor I and influence the synthesis of its oligosaccharide chains. J Immunol 1996;157:4963–9.

34. Clynes R, Takechi Y, Moroi Y, Houghton A, Ravetch JV. Fc receptors are required in passive and active immunity to melanoma. Proc Natl Acad Sci U S A 1998;95:652–6.

35. van De Winkel JG, Bast B, de Gast GC. Immunotherapeutic potential of bispecific antibodies. Immunol Today 1997;18:562–4.

36. Hamaguchi Y, Xiu Y, Komura K, Nimmerjahn F, Tedder TF. Antibody isotype-specific engagement of Fcγ receptors regulates B lymphocyte depletion during CD20 immunotherapy. J Exp Med 2006;203:743–53.

37. Platonov AE, Shipulin GA, Vershinina IV, Dankert J, van De Winkel JG, Kuijper EJ. Association of human Fcγ RIIa (CD32) polymorphism with susceptibility to and severity of meningococcal disease. Clin Infect Dis 1998;27:746–50.

38. Yuan FF, Wong M, Pererva N, et al. FcγRIIA polymorphisms in *Streptococcus pneumoniae* infection. Immunol Cell Biol 2003;81:192–5.

39. Lefranc MP, Giudicelli V, Kaas Q, et al. IMGT, the international ImMunoGeneTics information system. Nucleic Acids Res 2005;33:D593–7.